Spatial Organization of CaATPase Molecules in Sarcoplasmic Reticulum Vesicles†

Stefan Highsmith* and Joel A. Cohen

Departments of Biochemistry and Physiology, University of the Pacific, San Francisco, California 94115

Received August 13, 1986; Revised Manuscript Received September 30, 1986

ABSTRACT: Fluorescence intensity, polarization, and (Ca^{2+}-Mg^{2+})-ATPase (CaATPase) activity were measured for sarcoplasmic reticulum (SR) CaATPase with varying amounts of fluorescein isothiocyanate (FITC) attached at a specific site at or near the ATP binding site. The stoichiometry of attached FITC was proportional to the inhibition of ATPase activity, consistent with the independent labeling of one FITC site per CaATPase molecule. Polarization measurements on vesicular CaATPase indicated the occurrence of energy-transfer depolarization that increased as the fraction of binding sites labeled by FITC increased. Addition of the nonionic detergent dodecyl nonaoxyethylene alcohol ($C_{12}E_9$) eliminated the energy-transfer depolarization for all degrees of labeling with little direct effect on the attached FITC molecule. Fluorescence polarization measurements on sizing-column-purified FITC-labeled CaATPase in the presence of 30 mM $C_{12}E_9$ indicated that the sample consisted of homogeneous monomeric CaATPase. The attached FITC molecule was not sensitive to the bulk viscosity for either the vesicular or the detergent-solubilized CaATPase. The midpoints of the transition from vesicular to monomeric CaATPase as a function of increasing detergent concentration were determined from fluorescence polarization and light-scattering measurements. The dependence of these midpoints on the CaATPase concentration indicated a stoichiometry of 262 ± 35 molecules of $C_{12}E_9$ per CaATPase in the detergent–protein complex. Both measurements gave the same result. The decrease of fluorescence polarization with increasing saturation of the FITC binding sites for vesicular and detergent-solubilized CaATPase was analyzed in terms of energy-transfer depolarization to determine the spatial arrangements of CaATPase molecules. The statistically best fit to the data for the vesicular case was obtained by using a model in which each CaATPase has three neighboring CaATPase molecules, consistent with tetrahedra or two-stranded ribbons of CaATPases. The average distance between FITC molecules in this model was found to be 4.4 nm. The detergent-solubilized CaATPase was clearly monomeric.

The (Ca^{2+}-Mg^{2+})-ATPase (CaATPase)[1] of skeletal muscle sarcoplasmic reticulum (SR) uses MgATP as an energy source to pump Ca^{2+} out of the cytosol and into the SR lumen. The observation that two Ca^{2+} ions are transported for each ATP hydrolyzed (Hasselbach & Makinose, 1963; Weber et al., 1966) has been confirmed by many workers. More recently, studies have indicated that two Ca^{2+} ions and one MgATP are substrates for one CaATPase molecule (Møller et al., 1980; Murphy et al., 1982; Kosk-Kosicka et al., 1983), although this stoichiometry is not universally accepted. Less clear is the role that aggregation of CaATPase monomers into oligomers may have in Ca^{2+} transport. The SR membrane is rich in CaATPase, about 2:1 protein to lipid by weight (Stewart & MacLennan, 1974), with much of the protein being CaATPase (Meissner et al., 1973; Coll & Murphy, 1984; Barrabin et al., 1984), so there is little doubt that the CaATPase molecules are near one another. However, whether there are interactions between CaATPase monomers—either monomer–monomer binding in preferred spatial orientations or functional intermolecular interactions—has not been established.

Several lines of physical evidence indicate that there is, at least, association between monomeric subunits. Early electron microscopic studies showed there are about 4 times as many protein projections on the outside of SR vesicles as there are protein core structures in the lipid leaflet (Jilka et al., 1975; Scales & Inesi, 1976). That the CaATPase subunits are close enough to interact physically has been shown by chemical cross-linking (Murphy, 1976; Louis & Holroyd, 1978; Kosk-Kosicka et al., 1983), by fluorescence energy transfer (Vanderkooi et al., 1977; Watanabe & Inesi, 1982; Champeil et al., 1982; Fagan & Dewey, 1986), by excimer formation (Ludi & Hasselbach, 1983), and by concentration depolarization of fluorescence (Ludi & Hasselbach, 1982). The subunit proximity indicated by these results usually has been interpreted in terms of CaATPase dimers or tetramers.

Vanadate has been shown to cause several striking structural effects on the CaATPase (Dux & Martonosi, 1983; Taylor et al., 1984; Scales & Highsmith, 1984; Highsmith et al., 1985; Dux et al., 1985), and although millimolar vanadate is far from physiological, X-ray scattering from vandate-treated SR suggests that the subunits are in specific spatial orientations. The subunits appear strongly connected as dimers with weaker but definite interdimer connections to form rows or ribbons of CaATPase dimers (Taylor et al., 1984). Rows of CaATPase subunits have also been observed in the absence of vanadate in freeze–fracture electron micrographs of native CaATPase (Castellani et al., 1985) and of reconstituted

† This work was supported by NIH Grants AM 25177 and GM 35241 and by the American Heart Association with contributions from the San Francisco Chapter of the California Affiliate.

* Address correspondence to this author at the Department of Biochemistry, University of the Pacific.

[1] Abbreviations: SR, sarcoplasmic reticulum from skeletal muscle; CaATPase, (Ca^{2+}-Mg^{2+})-ATPase from SR; FITC, fluorescein isothiocyanate; $C_{12}E_9$, dodecyl nonaoxyethylene alcohol; P, polarization; A, emission anisotropy; EGTA, ethylene glycol bis(β-aminoethyl ether)-N,N,N',N'-tetraacetic acid; θ_e, effective angle between the donor emission and acceptor absorption dipoles; r_e, effective distance between a donor and acceptor; k_T, rate constant for energy transfer; k_F, rate constant for fluorescence; R_0, critical distance for a donor–acceptor pair; MOPS, 3-(N-morpholino)propanesulfonic acid.

0006-2960/87/0426-0154$01.50/0

CaATPase (Lentz et al., 1985).

The evidence that the subunits interact functionally is not as strong. The biphasic kinetics of Ca^{2+} binding and/or release (Ikemoto et al., 1981; Kurobe et al., 1983) require that each CaATPase have only one Ca^{2+} binding site in order to signify that the subunits interact. The observations that in the presence of detergents more than one CaATPase per functional unit is needed for full activity (LeMaire et al., 1976) and for the maintenance of cooperative Ca^{2+} binding and ATP regulatory effects (Silva & Verjovski-Almeida, 1983; Verjovski-Almeida & Silva, 1981) suggest the occurrence of functional subunit interactions but are not consistent with the larger body of evidence on detergent-solubilized CaATPase monomer that is discussed below. Target-theory studies of vesicular SR suggest a functional CaATPase dimer (Hymel et al., 1984). Finally, the observation that at alkaline pH the Hill coefficient for Ca^{2+} binding to vesicular SR is greater than 2 (Watanabe et al., 1981) suggests that at least two subunits can interact functionally.

There is a substantial amount of evidence in favor of a monomeric CaATPase pump. Nonionic detergents dissociate SR proteins and lipids into CaATPase monomers, in detergent micelles, which have full Ca^{2+}-activated ATPase activity (Dean & Tanford, 1978; Møller et al., 1980). Furthermore, the dependence of the monomer activity on free calcium (Murphy et al., 1982; Kosk-Kosicka et al., 1983; Scofano et al., 1985) is cooperative, as is Ca^{2+} binding to vesicular CaATPase (Inesi et al., 1980; Highsmith, 1982; Scofano et al., 1985). The feasibility of the monomer as the pump, based on its various properties, has been studied in detail by Møller and his associates (Møller et al., 1980, 1982; Andersen et al., 1982, 1985; Vilsen & Andersen, 1986), and a strong argument has been made in favor of a monomeric pump. The drawback to conclusions based on results from detergent-solubilized monomers is that these monomers cannot actually pump, since there is no membrane to provide compartments. In addition, there are questions regarding the completeness of monomerization in the presence of detergents (Silva & Verjovski-Almeida, 1983, 1985). Evidence that the monomeric CaATPase is the pump is provided by X-ray scattering measurements on membranes that are pumping, which suggest that the monomer is the major species (Brady et al., 1981).

On the whole, there are insufficient data to conclude whether the pumping unit is or is not oligomeric. In this work, keeping in mind the distinctions between (1) proximity of subunits with no interactions, (2) binding of subunits to form discrete aggregates with no functional interactions, and (3) binding of subunits that have functional interactions between ligand binding sites on different CaATPase molecules, we measured the fluorescence intensity and emission anisotropy of SR vesicles labeled at or near the ATP binding site with various amounts of fluorescein isothiocyanate (FITC). The data were not consistent with isolated CaATPase monomers or dimers. The best model, for the data obtained here, is one in which every CaATPase molecule has three neighboring CaATPase molecules. The results suggest that the CaATPase molecules exist in clusters, but there was no evidence of functional interactions between CaATPase neighbors.

Materials and Methods

Vesicular SR CaATPase was prepared (Eletr & Inesi, 1972) from rabbit hind leg muscle and stored at 0 °C in solutions containing 30% sucrose by weight. Protein concentrations were determined by using a biuret method and standardizing with isolated SR protein that was extracted from vesicles. Chemicals were reagent grade. Sucrose was ultrapure from Schwarz/Mann. The nonionic detergent $C_{12}E_9$ was purchased from Sigma Chemical Co.

Ca^{2+}-activated ATPase activities were measured at 25 °C by detecting inorganic phosphate production (Murphy, 1981). Rates were determined from slopes of plots of $[P_i]$ vs. time that had five points and linear regression r values of at least 0.99. Vesicular activities were determined for solutions containing 0.01 mg/mL SR protein in 63 mM KCl, 5 mM $MgCl_2$, 2 mM ATP, 0.83 mM EGTA, 1.0 mM $CaCl_2$, 4 mM MOPS (pH 7.0), and 1 μg/mL A23187. Detergent-solubilized CaATPase activities were measured with 30 mM $C_{12}E_9$ in the assay buffer and were calibrated by using a standard curve produced with the appropriate $[C_{12}E_9]$ in the phosphomolybdate solution.

Vesicular CaATPase was modified with FITC as described (Highsmith, 1984) at pH 7.7, 25 °C, and also at pH 7.7, 0 °C, for up to 18 h, as described under Results and Discussion. The FITC-modified SR vesicles were purified by size-exclusion chromatography with a Bio-Gel P-10 column (10 cm × 1 cm) or by centrifugation and resuspension of the pellet, with equivalent results. The protein concentration of the isolated modified SR was measured by either a biuret method or the Bradford method (Bradford, 1976), with equivalent results. The attached FITC did not affect the protein concentration determination, using unlabeled SR vesicles as a standard. Column-purified $C_{12}E_9$-solubilized CaATPase was prepared by using a 12 cm × 1 cm column packed with Sephacryl S-1000. The extent of FITC labeling was assayed by Ca^{2+}-activated ATPase activity (Highsmith, 1984).

Fluorescence intensity from FITC-labeled CaATPase was determined by using a Perkin-Elmer MPF-44B fluorospectrophotometer, irradiating the samples at 450 nm and observing at 520 nm without filters or polarizers. Light-scattering contributions to the fluorescence were negligible for these conditions. Polarizations were determined by using excitation and emission wavelengths of 490 and 520 nm, respectively, and the equation:

$$P = \frac{I_{0,0} - I_{0,90}(I_{90,0}/I_{90,90})}{I_{0,0} + I_{0,90}(I_{90,0}/I_{90,90})}$$

where $I_{x,y}$ values are the fluorescence intensities with the excitation and emission polarizers set at x and y degrees from the plane of the exciting light, respectively. Each $I_{x,y}$ for FITC-labeled CaATPase was corrected by subtracting the $I_{x,y}$ obtained with unmodified CaATPase at the same concentration. Emission anisotropies, which are additive for heterogeneous samples (Weber, 1952), were calculated as $A = (1/P - 1/3)^{-1}$.

Light-scattering measurements were made on unlabeled and FITC-labeled CaATPase samples using 350-nm light and detecting at 90° from the incident beam.

Results and Discussion

Fluorescence Intensity and CaATPase Activity Measurements on Vesicular and Solubilized FITC-Labeled CaATPase. Vesicular SR CaATPase was labeled with FITC and separated from free FITC as described above. The fluorescence intensity at 520 nm for the isolated FITC-labeled CaATPase is shown as a function of inhibition of CaATPase activity in Figure 1. The intensity of the attached probe is proportional to the inhibition, which is consistent with earlier measurements (Mitchinson et al., 1982; Andersen et al., 1982; Highsmith, 1984). Complete inhibition is obtained with 5.2–5.3 nmol of FITC/mg of SR protein (Highsmith & Murphy, 1984; Highsmith, 1984). The straight line in Figure 1 fits data obtained for labeling with variable amounts of FITC at 25 °C,

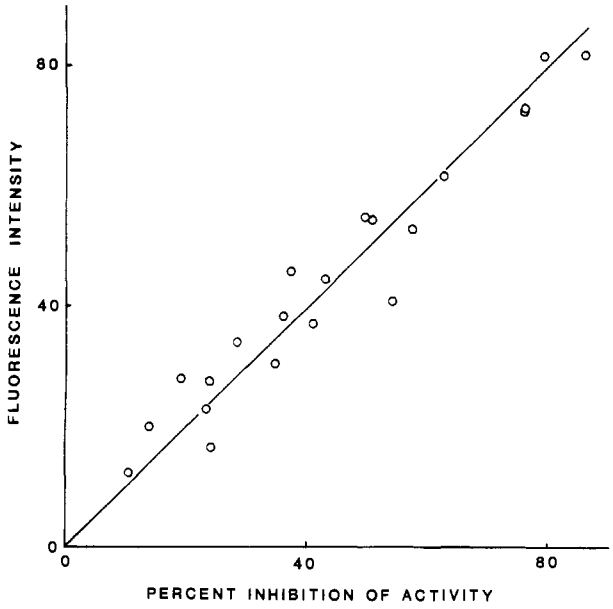

FIGURE 1: Vesicular CaATPase was modified with varying amounts of FITC and separated from any unreacted FITC as described under Materials and Methods. The relative intensity of the FITC fluorescence for 0.05 mg of protein/mL is plotted against the loss of Ca-activated ATPase activity at 25 °C. These data are consistent with reactive sites for FITC that do not interact with one another. The slope of the line is 1.0.

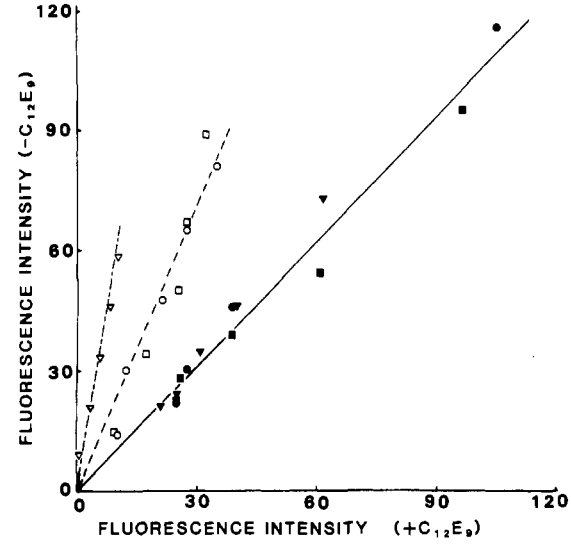

FIGURE 2: Vesicular CaATPase was modified with varying amounts of FITC and purified by size-exclusion chromatography or centrifugation. The FITC fluorescence intensity was then measured for 0.05 mg/mL samples with 0.1–4.8 nmol of FITC/mg of protein in buffer (100 mM KCl, 5 mM $MgCl_2$, 0.10 mM $CaCl_2$, and 10 mM MOPS) with and without 30 mM $C_{12}E_9$ at pH 6 (▼), 7 (■), and 8 (●). Parallel measurements were made on comparable concentrations of FITC in the absence of SR in solutions with and without 30 mM $C_{12}E_9$ at the same pHs (open symbols). Within experimental error, there is no unattached fluorescent FITC in the FITC–CaATPase preparations. The slope of the solid line is 1.03.

pH 7.7, with 0.1 mM $CaCl_2$ or 1 mM EGTA present, and at 0 °C, pH 7.7, with 0.1 mM $CaCl_2$ present, in the labeling incubation mixture. Pick and others have shown that FITC binds at or near the ATPase binding site specifically and stoichiometrically (Pick & Bassilian, 1981; Highsmith, 1984; Coll & Murphy, 1984). Recently, its site of attachment has been assigned to Lys-514 (MacLennan et al., 1985). FITC attached to the CaATPase is sensitive to protein conformation and responds to intramolecular ligand binding (Pick & Bassilian, 1981; Pick, 1981; Highsmith, 1986). Since fluorescence is sensitive to environment, the intensity of the FITC fluorescence could monitor interactions between ATP binding sites, if the subunits were interacting. However, the data in Figure 1 are fully explained by the simpler model of independent FITC attachment at noninteracting ATP-hydrolyzing sites. This does not exclude the possibility that ATP binding itself could involve subunit interactions, but the results shown in Figure 1 provide no evidence that the Lys-514 environment on one CaATPase is modified by FITC on another CaATPase.

Labeling of CaATPase molecules does not appear to affect the enzyme beyond blocking the binding of ATP and therefore inhibiting its ATPase activity. The hydrolytic activity for smaller substrates that do not require binding in the adenine subsite is not changed by FITC (Pick & Bassilian, 1981). The FITC–CaATPase molecules have the same appearance in negatively stained electron micrographs as unlabeled CaATPase (Highsmith et al., 1985; Coan et al., 1986) and form the same two-dimensional arrays when treated with vanadate (Highsmith et al., 1985).

It is crucial for polarization measurements that the samples be free of any unattached FITC. To test the effectiveness of the size-exclusion chromatography in removing free FITC, advantage was taken of the intensity loss that occurs in nonionic detergents for free FITC but not FITC–CaATPase. Identical aliquots of 0.05 mg/mL SR protein with 0.1–4.8 nmol of FITC/mg of SR protein were diluted in buffers at pH 6, 7, or 8 containing 0 or 30 mM $C_{12}E_9$. Parallel measurements were made on equivalent concentrations of FITC without SR present (Figure 2). The unattached probe fluorescence intensity is decreased 2.5-fold at pH 7 or 8, and 6-fold at pH 6, by the presence of the detergent micelles. This is probably because the micellar environment favors the monoanionic FITC which has a lower quantum yield than the dianion (Leonardt et al., 1971). The fluorescence intensity of the FITC–CaATPase samples was not sensitive to detergent, within experimental error. This result (Figure 2) indicates there is negligible fluorescent FITC that is not bound covalently to the CaATPase after the purification step. Moreover, the linearity of the data in Figure 1 suggests that all the FITC is bound in a homogeneous environment. These results strengthen the conclusion that FITC stoichiometrically modifies the CaATPase (Mitchinson et al., 1982; Andersen et al., 1982). The data in Figure 2 also indicate that the bound FITC is in an environment that is partially protected from the bulk solvent, in agreement with results from recent Stern–Volmer quenching studies (Highsmith, 1986).

Disparate reports regarding the degree of activation of CaATPase upon complete solubilization by nonionic detergents (Andersen et al., 1983; Dean & Tanford, 1978; Verjovski-Almeida & Silva, 1981; Kosk-Kosicka et al., 1983; LeMaire et al., 1976; Murphy et al., 1982; MacIntosh & Davidson, 1984; Martins & deMeis, 1985) stimulated a reinvestigation of the effects of $C_{12}E_9$ on activity. The CaATPase activities in the presence of 30 and 0 mM $C_{12}E_9$, respectively, had a ratio of 1.15 ± 0.12 under conditions (see Materials and Methods) in which A23187 was present and the high-affinity Ca^{2+} binding sites and the ATP-hydrolyzing and regulatory sites were saturated. The observed detergent activation is small, nearly zero within experimental error, and supports the conclusion that detergent activation of SR vesicle CaATPase activity by $C_{12}E_9$ is due to increased leakiness rather than any direct detergent–protein interaction (Murphy et al., 1982).

Fluorescence Polarization Measurements. In general, for conditions that maintain noninteracting fluorophores, the fluorescence polarization of a solution is independent of

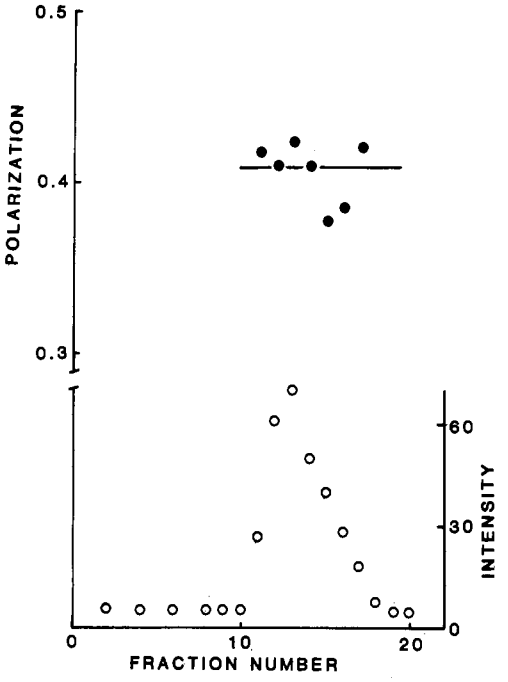

FIGURE 3: Vesicular CaATPase was modified with 4.2 nmol of FITC/mg of protein, solubilized with 30 mM $C_{12}E_9$, and eluted on a Sephacryl S-1000 column (1 × 12 cm) equilibrated with 100 mM KCl, 5 mM $MgCl_2$, 0.10 mM $CaCl_2$, 10 mM MOPS (pH 7.0, KOH), and 30 mM $C_{12}E_9$ at 25 °C. Each fraction (void volume is fraction 7) was analyzed for fluorescence intensity and polarization. There is evidence of tailing, but the polarization is constant, within experimental error, across the peak. [SR] ~ 0.05 mg/mL.

fluorophore concentration. However, when fluorophores are near one another, energy transfer can occur. FITC is an excellent fluorescence energy-transfer donor and acceptor, with a critical distance of 5.0 nm determined by energy-transfer depolarization (Förster, 1948). The dependence of polarization on the distance and the angle between the donor–emission and acceptor–absorption dipoles makes FITC polarization useful as a monitor of proximity and orientation. The polarization of CaATPase modified with 4.2 nmol of FITC/mg of protein and solubilized with 30 mM $C_{12}E_9$ is shown in Figure 3 for each fraction collected after elution on a size-exclusion column. The absence of any significant change in polarization with elution volume indicates there is a negligible fraction of solubilized material for which the FITC molecules are less than 6 nm apart, assuming a value of 0.67 for the orientation factor and that efficiencies as low as 25% are detectable. This result and those in Figures 1 and 2 suggest that a homogeneous sample of monomeric FITC-labeled detergent-solubilized CaATPase has been prepared. There are no indications of unattached FITC in the column-purified vesicular samples or of heterogeneity of the detergent-solubilized samples.

The polarization of vesicular FITC-CaATPase decreases with increasing saturation of FITC labeling. Shown in Figure 4A are results for SR CaATPase labeled with 0.15–4.6 nmol of FITC/mg of SR protein, ranging from 3% to 87% saturation of the total FITC binding sites. That this decrease in polarization is due to proximity is demonstrated in Figure 4B where the polarization is shown for the same FITC–CaATPase preparations in solutions containing 30 mM $C_{12}E_9$. Solubilization of the CaATPase reduces its rotational correlation coefficient from over 100 μs to about 0.2 μs at 25 °C (Thomas & Hidalgo, 1978; Murphy et al., 1982). However, the excited-state lifetime of the FITC–CaATPase is 4.0 ns (Highsmith, 1986), so the increase in the rate of rotational Brownian motion of the CaATPase upon solubilization does not affect the polarization detected with FITC. The small

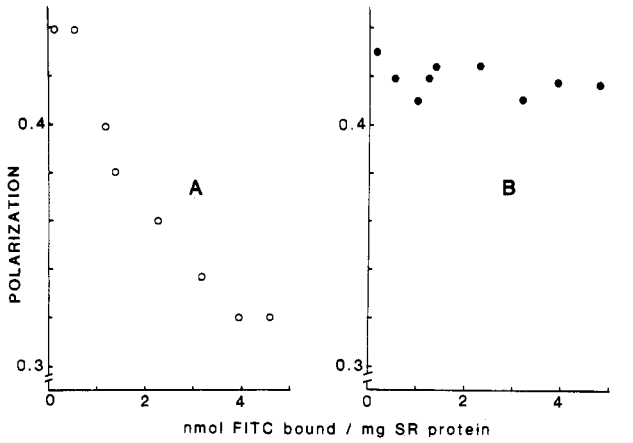

FIGURE 4: Polarization of FITC-labeled SR CaATPase is shown as a function of increasing amount of attached FITC for (A) vesicular and (B) 30 mM $C_{12}E_9$-solubilized enzyme. The decrease in polarization in panel A is due to fluorescence energy-transfer depolarization (see text). [SR] = 0.05 mg/mL.

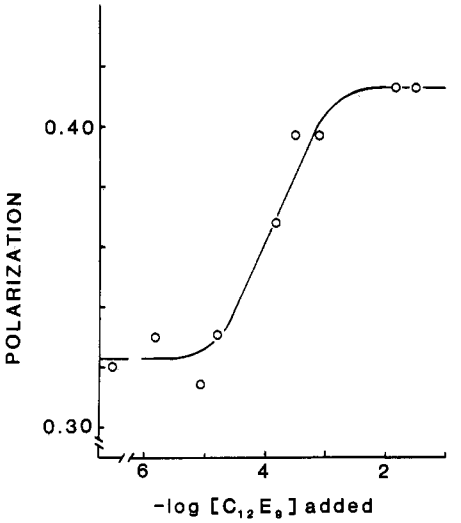

FIGURE 5: Polarization of CaATPase modified with 4.8 nmol of FITC/mg of SR protein is shown for 0.05 mg of SR/mL in pH 7 buffer (see Figure 2 caption) containing increasing amounts of $C_{12}E_9$.

difference between the polarization of the fully labeled detergent-solubilized CaATPase and that of the minimally labeled vesicular CaATPase, for which the probability of FITC–FITC neighbors is small, supports the conclusion that high concentrations of $C_{12}E_9$ monomerize the enzyme (Murphy et al., 1982; Coll & Murphy, 1984). The data in Figures 1 and 2 suggest that no cooperative binding of FITC is occurring and that $C_{12}E_9$ does not change the excited-state lifetime of the attached FITC. This leaves energy transfer as the most likely mechanism for the observed depolarization. Energy transfer between labeled vesicular CaATPase molecules was originally observed by Vanderkooi et al. (1977).

The effect of increasing amounts of $C_{12}E_9$ on the polarization of FITC–CaATPase with 4.8 nmol of FITC/mg of SR protein is shown in Figure 5. This ability of detergents to separate CaATPase molecules has been monitored previously by fluorescence energy transfer between heterogeneous donor–acceptor pairs (Vanderkooi et al., 1977; Watanabe & Inesi, 1982), by the loss of eximer formation (Ludi & Hasselbach, 1982), by increased rates of the rotation of covalently attached pyrene (Ludi & Hasselbach, 1983), and by light scattering (Champeil et al., 1982).

The $[C_{12}E_9]$ at the midpoint of the transition from lower to higher polarization (Figure 5) increased with increasing

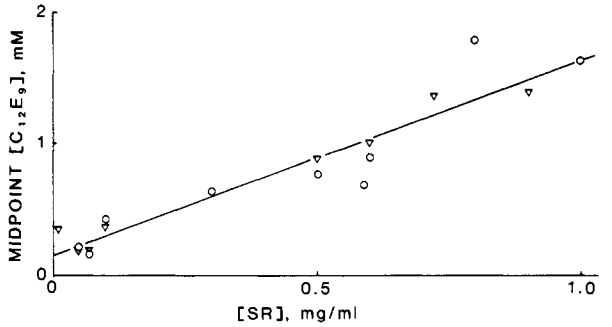

FIGURE 6: Midpoints for the increase in FITC–CaATPase polarization (○) or the decrease in 350-nm light scattering (▽) due to increasing [$C_{12}E_9$] are plotted against the concentration of SR protein in 100 mM KCl, 5 mM $MgCl_2$, 0.10 mM $CaCl_2$, and 10 mM MOPS (pH 7.0, KOH).

[SR]. A plot of $[C_{12}E_9]_{1/2}$ vs. [SR] is shown in Figure 6, along with complementary data obtained from the decrease in light scattering as [$C_{12}E_9$] is increased (titrations not shown). The data were fit to the expression:

$$[C_{12}E_9]_{1/2,\text{total}} = [C_{12}E_9]_{1/2,\text{free}} + n[\text{DSR}]$$

where the subscript $^1/_2$ denotes the midpoint, and n is the number of $C_{12}E_9$ molecules bound to a solubilized CaATPase in the complex DSR. The slope of the fitted line in Figure 6 yields n = 0.82 g of $C_{12}E_9$/g of protein or 262 ± 35 molecules of $C_{12}E_9$/CaATPase, using 5.3 nmol of CaATPase/mg of SR protein. These values are consistent with those obtained with the similar detergent $C_{12}E_8$: 0.83 g/g (Dean & Tanford, 1978) and 1 g/g (Andersen et al., 1983).

The polarization for the lowest degree of labeling of the vesicular CaATPase is 0.44 (Figure 4), which approaches the maximum theoretical value of 0.50, suggesting that the probe is motionally restricted. Perrin plots for vesicular FITC–CaATPase in the presence of EGTA, Ca^{2+}, and phosphate or vanadate, and in solutions containing $C_{12}E_9$, are shown in Figure 7A–D. There is little dependence of P^{-1} on T/η, suggesting that the FITC is in an environment that is not sensitive to the viscosity of the bulk solvent. Shown in Figure 7E are data for free FITC. The value of the intrinsic polarization, P_o, obtained by extrapolation, is 0.49, which is close to the theoretical maximum. Weber (1966) has shown that the P_o values of probes attached to proteins can be used to determine an equivalent cone-shaped volume in which the probe is free to move, using the equation:

$$P_o = P_{\max}(3\cos^2\theta_c - 1)/2 \quad (1)$$

where P_o is the observed value from the Perrin plot extrapolation, $P_{\max}$ is the value obtained when all motion is stopped, and θ_c is the full angle of the cone. Using values from extrapolations of the data in Figure 7A for P_o and from Figure 7E for $P_{\max}$, we estimate θ_c to be 16 ± 5°. There are no data near T/η = 0 in Figure 7A, so the uncertainty associated with this estimate is large, but it suggests that the probe has only limited freedom of rotation and therefore is in a sterically hindered environment. This is consistent with the conclusions drawn from recent Stern–Volmer quenching measurements on FITC-labeled vesicular CaATPase (Highsmith, 1986).

Analysis of Fluorescence Energy-Transfer Depolarization Data. Energy-transfer depolarization provides information on the distance between the donor and acceptor, and on the angle between the donor emission dipole and the acceptor absorption dipole (Weber & Daniel, 1966; Knox, 1968; Dale & Eisinger, 1974). The experimentally determined decrease in emission anisotropy that occurred with increasing saturation of the FITC labeling sites was compared to the decreases predicted from models of various CaATPase spatial arrangements, based upon a theory by Weber and Daniel (1966). The emission anisotropies are calculated from

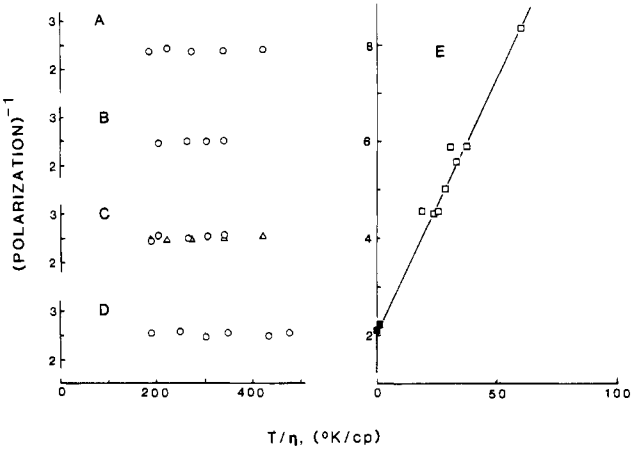

FIGURE 7: Reciprocal polarization vs. T/η plots for FITC–CaATPase (1.0 nmol of FITC/mg of SR protein) in 100 mM KCl, 5 mM $MgCl_2$, and 10 mM MOPS are shown on the left for samples with (A) 1 mM EGTA and 20 mM phosphate (pH 6), (B) 1 mM EGTA and 0.25 mM vanadate, (C) 0.10 mM $CaCl_2$ (○) or 1.0 mM $CaCl_2$ (△), and (D) 0.10 mM $CaCl_2$ and 30 mM $C_{12}E_9$. Temperature was changed to alter viscosity. On the right side (E) is shown P^{-1} vs. T/η for free FITC. The closed symbols are for data obtained by using 30% sucrose to vary η. The open symbols are for CaATPase in 100 mM KCl, 5 mM $MgCl_2$, 0.10 mM $CaCl_2$, and 10 mM MOPS (pH 7.0, KOH) at different temperatures.

$$A_{\text{calcd}} = \sum_{i=0}^{q} \phi_i A_i \quad (2)$$

where ϕ_i is the fractional fluorescence intensity and A_i is the emission anisotropy, for each fluorescent species. In the model used here, the various fluorescent species differ in the number of neighboring fluorophores that are adjacent to each fluorescent donor. This number can range from 0 to q, where q is the coordination number of the geometric arrangement of fluorophore binding sites, i.e., the number of sites that are nearest neighbors to each site.

By use of notation similar to that of Weber and Daniel (1966), the A_i are made up of contributions from A_0, where there is no energy transfer, and A_T, where transfer occurs, weighted by the probabilities of transfer, P_i, where

$$P_i = (ik_T/k_F)/(1 + ik_T/k_F) \quad (3)$$

The expression for A_{calcd} is

$$A_{\text{calcd}} = \sum_{i=0}^{q} \phi_i[A_0 - (A_0 - A_T)P_i] \quad (4)$$

which is a function of the number of neighboring acceptors (i) for each donor (where $0 \le i \le q$), the rate constants for fluorescence and transfer (k_F and k_T, respectively), the effective angle between the emission and absorption dipoles (θ_e), the effective distance between the dipoles (r_e), the critical distance for the donor–acceptor pair (R_0), and the emission anisotropy when the system is saturated (A_S). Weber and Daniel (1966) also derived the following relationships, assuming that multiple transfers may be ignored:

$$A_T = A_0(3\cos^2\theta_e - 1)/2 \quad (5)$$

$$(A_0 - A_S)/(A_S - A_T) = qk_T/k_F \quad (6)$$

and

$$k_T/k_F = \cos^2\theta_e(R_0/r_e)^6 \quad (7)$$

From Figure 1, it is seen that the fluorescence intensity is proportional to the FITC-induced loss of CaATPase activity, which in turn is proportional to the fractional saturation of FITC binding sites, f. Thus, for any f, if we assume the sites

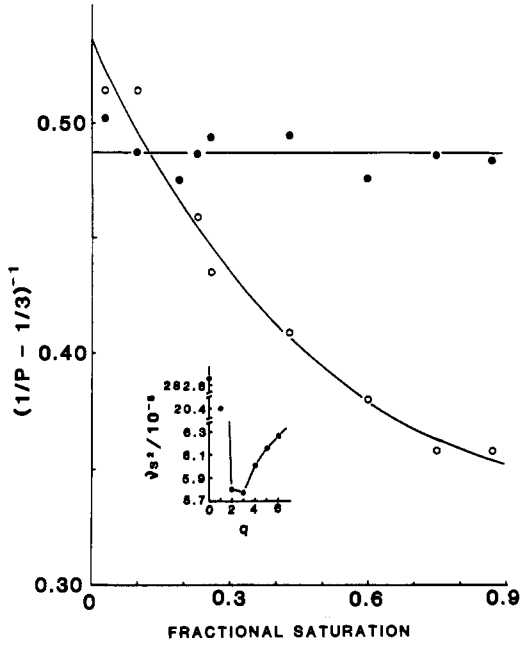

FIGURE 8: Polarization data, as in Figure 4, replotted for vesicular (O) and solubilized (●) FITC–CaATPase as emission anisotropies vs. degree of labeling. Data were fit by the model described in the text. The solid lines are the fits for $q = 3$ (vesicular case) and $q = 0$ (solubilized case). The inset shows the relative goodness of fits to the vesicular FITC–CaATPase data for various values of q, expressed as νs^2 vs. q, where ν is the number of degrees of freedom and s^2 is the variance of each fit. νs^2 equals the sum of the squares of the residuals for each fit.

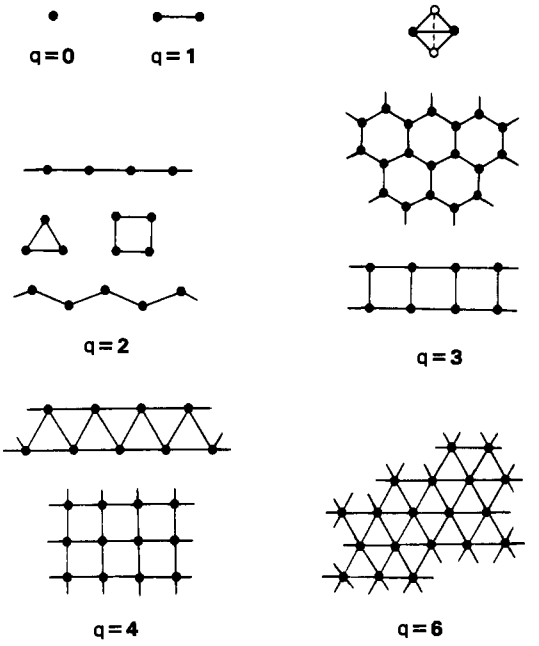

FIGURE 9: Spatial arrangements of FITC molecules are shown for various values of q (=number of neighbors) based on the model described in the text. Each FITC is represented by a closed circle, and lines connect neighbors. The tetrahedron is the only isolated oligomeric structure that has $q = 3$ and equidistant neighbors. The array and double-stranded ribbon structures extend indefinitely.

are labeled randomly, the value for the fractional fluorescence intensity of each species, ϕ_i in eq 2, can be calculated from the statistics of random distributions:

$$\phi_i = \binom{q}{i} f^i (1-f)^{q-i} \tag{8}$$

where $\binom{q}{i}$ is the binomial coefficient $q!/[i!(q-i)!]$ and $0 \leq i \leq q$. The right side of eq 8 is the probability, for a given donor, that i neighboring sites are occupied by fluorophores and that $q - i$ neighboring sites are not occupied by fluorophores, where the fraction of total sites occupied by fluorophores is f, and $0 \leq f \leq 1$. Thus, for a given f, ϕ_i is the fraction of total fluorophores that have i neighboring fluorophores.

The geometric modeling of CaATPase spatial arrangements is now done as follows. The data of emission anisotropy vs. f (Figure 8) are analyzed by use of eq 2. In eq 2, A_i is expressed, for each value of i, in terms of A_0, A_T, A_S, and q by use of eq 3, 4, and 6. Also, ϕ_i is expressed as a function of f, for each value of i, in terms of q by use of eq 8. Thus, A_{calcd} can be written as a function of f in terms of the parameters A_0, A_T, A_S, and q. Since q is restricted to integral values, it is not possible to determine the best values of A_0, A_T, A_S, and q simply by a four-parameter fit to the data of emission anisotropy vs. f. Our procedure is to specify the various integral values of q, and for each value to perform a three-parameter fit for the optimal values of A_0, A_T, and A_S. The variances of the fits then indicate which value of q is best. The nonlinear least-squares fits were performed by use of the Marquardt algorithm, which combines gradient-search and matrix-inversion methods (Bevington, 1969).

Figure 8 shows the best fits of eq 2 to the data for vesicular and detergent-solubilized FITC–CaATPase. For the vesicular case, the best fit is obtained with $q = 3$, where $A_0 = 0.54$, $A_T = 0.31$, and $A_S = 0.35$. In the inset of Figure 8 the product of the number of degrees of freedom and the variance of each fit is plotted against q. Although $q = 3$ gives a much better fit than $q = 0$ or 1, the fits obtained with $q = 2$–6 are only slightly worse than that obtained with $q = 3$. Fortunately, the physical parameters of interest here (A_0, r_e, and θ_e) are not very sensitive to q in the 2–6 range. The values $A_0 = 0.54 \pm 0.06$, $r_e = 4.4 \pm 0.5$ nm, and $\theta_e = 32 \pm 6°$ were obtained by using eq 5–7 and $R_0 = 5.0$ nm (Förster, 1948).

The $q = 3$ result is consistent with an arrangement of FITC binding sites in which each site has three equidistant neighboring sites. Some geometric arrangements of FITC molecules that fulfill this $q = 3$ criterion are pictured in Figure 9, e.g., isolated tetrahedra, extended hexagonal planar arrays, or extended ladderlike "ribbons". Also shown in Figure 9 are several geometric arrangements that are less compatible with the data. These include isolated monomers ($q = 0$), isolated dimers ($q = 1$), and the two-dimensional array for $q = 6$.

It should be appreciated that the modeling of possible arrangements of CaATPase molecules as arrays in which each CaATPase has q equidistant neighbors is only an approximation. Arrangements can also be imagined in which the neighbors are not equidistant or in which different sites have different numbers of neighbors. The sites could also be distributed randomly in the membrane, with no short- or long-range order at all. Our results should thus be interpreted in terms of *average* configurations that are not necessarily strictly geometrical. Therefore, $q = 3$ represents the average number of CaATPase molecules that are neighbors to each CaATPase, r_e is the average distance between neighboring FITC binding sites, and θ_e is the average angle between the donor emission and acceptor absorption dipoles.

Keeping the above limitations in mind, further discrimination between spatial arrangements can be made by comparing the area per CaATPase, obtained from the $q = 3$ lattice when $r_e = 4.4$ nm, to areas determined by others and to calculated areas. The two-dimensional arrays of CaATPase molecules that are induced by vanadate have been analyzed by Taylor et al. (1986), who obtained a surface lattice unit cell after image reconstruction which had a cross-sectional area per CaATPase of 36.9 nm^2. The unit cell area is about 50%

larger than the cross-sectional area of the CaATPase itself. This area is of interest here because it is for a case in which the CaATPase molecules are bound to one another. By comparison, the average area per CaATPase for randomly distributed molecules, with no binding, can be estimated by calculation (Scales & Inesi, 1976) using the vesicle volume (7.4 ± 0.2 mL/g of protein; Duggan & Martonosi, 1970), the vesicle radius (75 nm; Scales & Inesi, 1976), the percentage of total protein that is CaATPase (50% by weight; Coll & Murphy, 1984), and a molecular weight of 115 000 for the CaATPase. This calculation gives an area per CaATPase, averaged over the whole membrane, of 110 nm^2. Experimentally determined areas per CaATPase are substantially smaller (Napolitano et al., 1983; Franzini-Armstrong & Ferguson, 1985). The area per CaATPase obtained here from the fluorescence measurements is 25 nm^2 for the hexagonal ($q = 3$) lattice. This area is less than one-quarter of the average area per CaATPase calculated for randomly distributed molecules and is closer to the area for "crystallized" CaATPase. This result suggests that the FITC-labeled CaATPase molecules are clustered in the bilayer and therefore probably bind to one another. This conclusion is consistent with that of Franzini-Armstrong and Ferguson (1985), who did a stereological study of negatively stained SR vesicles and concluded that the CaATPase molecules exist as aggregates.

The value obtained for the effective angle between the donor emission and acceptor absorption dipoles, $\theta_e = 32 \pm 6°$, does not impose additional geometrical constraints on the possible arrangements of neighboring CaATPase molecules, given the apparent local freedom of motion for each FITC molecule ($\theta_c = 16 \pm 5°$, eq 1).

Within the present interpretational framework, and the assumptions of random labeling of FITC binding sites and neglect of multiple transfers (Weber & Daniel, 1966), there are three simple spatial arrangements that are compatible with the vesicular data: (1) tetrahedra, which could result from CaATPase tetramers whose subunits project different distances from the bilayer; (2) two-stranded ribbons; and (3) a hexagonal array (Figure 9, $q = 3$). Tetrameric clusters and two-stranded ribbons have been observed in negatively stained electron micrographs of vesicular SR (Jilka et al., 1975; Scales & Inesi, 1976; Taylor et al., 1984; Castellani et al., 1985). The data here do not permit distinction between these two arrangements or between them and the hexagonal array, as all are $q = 3$ configurations. However, these data do exclude lower orders of organization, such as isolated monomers or dimers. On the other hand, for the case of the detergent-solubilized FITC-labeled CaATPase, the only value for q that is consistent with the emission anisotropy data is zero. In this case, the plot of A_{calcd} vs. f is a horizontal line (Figure 8). This result supports the conclusion that the $C_{12}E_9$-solubilized CaATPase is monomeric (Murphy et al., 1982).

Acknowledgments

We thank Peggy Bloebaum and Douglas Barker for expert technical assistance, Professor A. J. Murphy for a critical reading of the manuscript, and Professor Nicholas Lange of the Massachusetts Institute of Technology Statistics Center for his expert advice.

References

Andersen, J. P., Møller, J. V., & Jorgensen, P. L. (1982) *J. Biol. Chem. 257*, 8300–8307.

Andersen, J. P., LeMaire, M., Kragh-Hansen, U., Champeil, Ph., & Møller, J. V. (1983) *Eur. J. Biochem. 1314*, 205–214.

Andersen, J. P., Lassen, K., & Møller, J. V. (1985) *J. Biol. Chem. 260*, 371–380.

Barrabin, H., Scofano, H., & Inesi, G. (1984) *Biochemistry 23*, 1542–1548.

Bevington, P. R. (1969) *Data Reduction and Error Analysis for the Physical Sciences*, p 237, McGraw-Hill, New York.

Bradford, M. M. (1976) *Anal. Biochem. 72*, 248–254.

Brady, G. W., Fein, D. B., Harder, N. E., Spehr, R., & Meissner, G. (1981) *Biophys. J. 34*, 13–34.

Castellani, L., Hardwicke, P. M. D., & Viber, P. (1985) *J. Mol. Biol. 185*, 579–594.

Champeil, P., Rigand, J. L., & Gingold, M. P. (1982) *Z. Naturforsch. C: Biosci. 37C*, 513–516.

Coan, C., Scales, D., & Murphy, A. J. (1986) *J. Biol. Chem. 261*, 10394–10403.

Coll, R., & Murphy, A. J. (1984) *J. Biol. Chem. 259*, 14249–14254.

Dale, R. E., & Eisinger, J. (1974) *Biopolymers 13*, 1573–1605.

Dean, W. L., & Tanford, C. (1978) *Biochemistry 17*, 1683–1690.

Duggan, P. F., & Martonosi, A. (1970) *J. Gen. Physiol. 56*, 147–159.

Dux, L., & Martonosi, A. (1983) *J. Biol. Chem. 258*, 2599–2603.

Dux, L., Taylor, K. A., Ting-Beall, H. P., & Martonosi, A. (1985) *J. Biol. Chem. 260*, 11730–11743.

Eletr, S., & Inesi, G. (1972) *Biochim. Biophys. Acta 282*, 174–179.

Fagan, M. H., & Dewey, T. G. (1986) *J. Biol. Chem. 261*, 3654–3660.

Förster, T. (1948) *Ann. Phys. (Leipzig) 2*, 55–75.

Franzini-Armstrong, C., & Ferguson, D. G. (1985) *Biophys. J. 48*, 607–615.

Hasselbach, W., & Makinose, M. (1963) *Biochem. Z. 339*, 94–119.

Highsmith, S. (1982) *Biochemistry 21*, 3786–3789.

Highsmith, S. (1984) *Biochem. Biophys. Res. Commun. 124*, 183–189.

Highsmith, S. (1986) *Biochemistry 25*, 1049–1054.

Highsmith, S., & Murphy, A. J. (1984) *J. Biol. Chem. 259*, 14651–14656.

Highsmith, S., Barker, D., & Scales, D. (1985) *Biochim. Biophys. Acta 817*, 123–133.

Hymel, L., Maurer, A., Berenski, C., Jung, C. Y., & Fleisher, S. (1984) *J. Biol. Chem. 259*, 4890–4895.

Ikemoto, N., Garcia, A. M., Kurobe, Y., & Scott, T. L. (1981) *J. Biol. Chem. 256*, 8593–8601.

Inesi, G., Coan, C., Lewis, D., & Kurzmack, M. (1980) *J. Biol. Chem. 255*, 3025–3031.

Jilka, R. L., Martonosi, A. M., & Tillack, T. W. (1975) *J. Biol. Chem. 250*, 7511–7524.

Knox, R. S. (1968) *Physica (Amsterdam) 39*, 361–386.

Kosk-Kosicka, D., Kurzmack, M., & Inesi, G. (1983) *Biochemistry 22*, 2559–2567.

Kurobe, Y., Nelson, R. N., & Ikemoto, N. (1983) *J. Biol. Chem. 258*, 4381–4389.

LeMaire, M., Møller, J. V., & Tanford, C. (1976) *Biochemistry 15*, 2336–2342.

Lentz, B. R., Clubb, K. W., Alford, D. R., Hochli, M., & Meissner, G. (1985) *Biochemistry 24*, 433–442.

Leonardt, H., Gordon, L., & Livingston, R. (1971) *J. Phys. Chem. 75*, 245–249.

Louis, C. F., & Holroyd, J. A. (1978) *Biochim. Biophys. Acta 535*, 222–232.

Ludi, H., & Hasselbach, W. (1982) *Z. Naturforsch. C: Biosci. 37C*, 1170–1179.
Ludi, H., & Hasselbach, W. (1983) *Eur. J. Biochem. 130*, 5–8.
MacIntosh, D. B., & Davidson, G. A. (1984) *Biochemistry 23*, 1959–1965.
MacLennan, D. H., Brandl, C. J., Korczak, B., & Green, N. M. (1985) *Nature (London) 316*, 696–700.
Martins, O. B., & deMeis, L. (1985) *J. Biol. Chem. 260*, 6776–6781.
Meissner, G., Conner, G. E., & Fleisher, S. (1973) *Biochim. Biophys. Acta 298*, 246–269.
Mitchinson, C., Wilderspin, A. F., Trinnaman, B. J., & Green, N. M. (1982) *FEBS Lett. 146*, 87–92.
Møller, J. V., Lind, K. E., & Andersen, J. P. (1980) *J. Biol. Chem. 255*, 1912–1920.
Møller, J. V., Mahrous, T. S., Andersen, J. P., & LeMaire, M. (1982) *Z. Naturforsch., C: Biosci. 37C*, 517–521.
Murphy, A. J. (1976) *Biochem. Biophys. Res. Commun. 70*, 160–166.
Murphy, A. J. (1981) *J. Biol. Chem. 256*, 12046–12050.
Murphy, A. J., Pepitone, M., & Highsmith, S. (1982) *J. Biol. Chem. 257*, 3551–3554.
Napolitano, C. A., Cooke, P., Segalman, K., & Herbette, L. (1983) *Biophys. J. 42*, 119–125.
Pick, U. (1981) *FEBS Lett. 123*, 131–136.
Pick, U., & Bassilian, S. (1981) *FEBS Lett. 123*, 127–130.
Scales, D., & Inesi, G. (1976) *Biophys. J. 16*, 735–751.
Scales, D., & Highsmith, S. (1984) *Z. Naturforsch. C: Biosci. 39C*, 177–179.
Scofano, H., Barrabin, H., Inesi, G., & Cohen, J. A. (1985) *Biochim. Biophys. Acta 819*, 93–104.
Silva, J. L., & Verjovski-Almeida, S. (1983) *Biochemistry 22*, 707–716.
Silva, J. L., & Verjovski-Almeida, S. (1985) *J. Biol. Chem. 260*, 4764–4769.
Stewart, P. S., & MacLennan, D. H. (1974) *J. Biol. Chem. 249*, 985–993.
Taylor, K., Dux, L., & Martonosi, A. N. (1984) *J. Mol. Biol. 174*, 193–204.
Thomas, D. D., & Hidalgo, C. (1978) *Proc. Natl. Acad. Sci. U.S.A. 75*, 5488–5492.
Vanderkooi, J. M., Ierokomas, A., Nakamura, H., & Martonosi, A. (1977) *Biochemistry 16*, 1262–1267.
Verjovski-Almeida, S., & Silva, J. L. (1981) *J. Biol. Chem. 256*, 2940–2944.
Vilsen, B., & Andersen, J. P. (1986) *Biochim. Biophys. Acta 855*, 429–431.
Watanabe, T., & Inesi, G. (1982) *Biochemistry 21*, 3254–3259.
Watanabe, T., Lewis, D., Nakamoto, R., Kurzmack, M., Fronticelli, C., & Inesi, G. (1981) *Biochemistry 20*, 6617–6625.
Weber, A., Herz, R., & Reiss, I. (1966) *Biochem. Z. 345*, 329–369.
Weber, G. (1952) *Biochem. J. 51*, 155–167.
Weber, G. (1966) in *Fluorescence and Phosphorescence Analysis* (Hercules, D. M., Ed.) pp 217–241, Wiley-Interscience, New York.
Weber, G., & Daniel, E. (1966) *Biochemistry 5*, 1900–1907.